Bachelor’s Thesis
TVVR 26/4001

Water balance study at a small-scale catchment

Zhuosong Wang

Division of Water Resources Engineering
Department of Building and Environmental Technology
Lund University

Water balance study at a small-scale catchment

By:
Zhuosong Wang

Bachelor's Thesis

Division of Water Resources Engineering
Department of Building & Environmental Technology
Lund University
Box 118
221 00 Lund, Sweden

Water Resources Engineering
TVVR-26/4001
ISSN 1101-9824

Lund 2026
www.tvrl.lth.se

Bachelor’s Thesis
Division of Water Resources Engineering
Department of Building & Environmental Technology
Lund University

Swedish title:	<Vattenbalansstudie vid ett småskaligt avrinningsområde>
English title:	<Water balance study at a small-scale catchment>
Author(s):	<Zhuosong Wang>
Supervisor:	<Linus Zhang>
Examiner:	<Jing Li>
Language	<English>
Year:	2026
Keywords:	<Water balance; Irrigation pond; Overflow analysis; Evaporation estimation; Flood mitigation>

Acknowledgements

During my four-month exchange period at Lund University, which began in January 2026, I was fortunate to receive support from many individuals who made this research and my stay possible.

My first days were eased by the local reception team — teachers and volunteers — whose dedication ensured my smooth transition into this new environment. They arranged temporary accommodation for me in Kävlinge, where I experienced the quiet beauty of the winter landscape and discovered unexpected hospitality from members of the local community, including the proprietress of a nearby restaurant who generously shared her insights into Swedish life, and the chef whose kind encouragement was greatly appreciated.

In February, I relocated to Lund, where Professor Linus Zhang and the teaching faculty provided invaluable academic support. Professor Zhang guided my thesis research while offering practical counsel on navigating daily life in this new environment. Despite initial language barriers, the classrooms became forums for vibrant academic exchange with international peers, and student association activities offered memorable moments that enriched my scholarly routine.

As coursework concluded, I also had the opportunity to visit Copenhagen during the Easter break, where I gained broader perspectives on Scandinavian culture and architecture, further enriching my international experience.

Though I arrived in Sweden alone, I never felt isolated throughout these months. To the reception team who welcomed me at Lund University, to Professor Zhang for shaping my academic path, and to the international community that became my home away from home—I extend my sincere and heartfelt gratitude.

Abstract

This study presents a comprehensive water balance analysis of an irrigation pond at Gårdstånga Nygård farm in southern Sweden, conducted over a 29-month period from June 2021 to October 2023. Utilizing continuous water level monitoring and regional meteorological observations, the research quantified key hydrological components including precipitation, catchment inflow, evapotranspiration, and overflow discharge calculated using an orifice-flow equation for the vertical pipe overflow structure. The analysis reveals distinct seasonal patterns and a dramatic hydrological intensification during 2023. Sustained overflow occurred during two main periods (September 2021–June 2022 and November 2022–October 2023), separated by a dry summer interval in 2022 when the water level fell below the overflow threshold. Total overflow over the 29-month period amounted to approximately 2.43 million cubic metres. Annual overflow increased markedly from 370×10^3 m^3 in 2021 to $1,331 \times 10^3$ m^3 in 2023, with the latter representing approximately 99.8% of the annual catchment inflow. The pond functioned primarily as a flow-through system during wet periods, with mean water levels rising from +0.20 m (2021) to +0.76 m (2023) relative to the overflow threshold. These findings demonstrate the pond's role as a multifunctional stormwater retention infrastructure, with the overflow structure controlling water levels to prevent agricultural flooding while the continuous overflow regime highlights the need for active water level management to preserve irrigation storage capacity. These results provide valuable insights for sustainable water resource management, agricultural infrastructure design, and climate adaptation strategies in Nordic agricultural settings.

Sammanfattning

Denna studie presenterar en omfattande vattenbalansanalys av en bevattningsdamm på Gårdstånga Nygård i södra Sverige, genomförd över en 29-månadersperiod från juni 2021 till oktober 2023. Genom kontinuerlig vattennivåövervakning och regionala meteorologiska observationer kvantifierade forskningen centrala hydrologiska komponenter inklusive nederbörd, tillflöde från avrinningsområdet, avdunstning och överflödesavledning beräknad med hjälp av en mynningsekvation för det vertikala rörets överflödesstruktur. Analysen avslöjar tydliga säsongsmässiga mönster och en dramatisk hydrologisk intensifiering under 2023. Långvarigt överflöde inträffade under två huvudsakliga perioder (september 2021–juni 2022 och november 2022–oktober 2023), åtskilda av en torr sommarperiod 2022 då vattennivån sjönk under överflödeströskeln. Den totala överflödesvolymen över 29-månadersperioden uppgick till cirka 2,43 miljoner kubikmeter. Årligt överflöde ökade markant från 370 × 10^3 m^3 under 2021 till 1 331 × 10^3 m^3 under 2023, vilket motsvarar cirka 99,8% av årets totala tillflöde. Dammen fungerade huvudsakligen som ett genomströmningssystem under våta perioder, med medelvattennivåer som steg från +0,20 m (2021) till +0,76 m (2023) relativt överflödeströskeln. Resultaten visar dammens roll som en multifunktionell stormvattenretentionsinfrastruktur, där överflödesstrukturen kontrollerar vattennivåerna för att förhindra jordbruksöversvämningar, medan det kontinuerliga överflödet understryker behovet av aktiv vattennivåhantering för att bevara bevattningslagringskapacitet. Dessa resultat ger värdefulla insikter för hållbar vattenresurshantering, jordbruksinfrastruktursdesign och klimatanpassningsstrategier i nordiska jordbruksmiljöer.

Table of contents

1 Introduction

1.1 Background and Context

Water is one of the most critical resources for agricultural production, and effective water management is essential for sustainable farming practices. In many regions, irrigation ponds serve as vital infrastructure for storing water during wet periods and supplying it during dry seasons. These small water bodies play a multifunctional role in agricultural landscapes, providing not only irrigation water but also contributing to flood control, groundwater recharge, and biodiversity conservation (Falkenmark and Rockström, 2006). Understanding the hydrological behavior of these ponds through water balance analysis is fundamental to optimizing their design and operation (Allen et al., 1998).

The water balance approach provides a quantitative framework for analyzing the inputs, outputs, and storage changes within a hydrological system. For small water bodies such as irrigation ponds, the water balance is particularly sensitive to local climatic conditions, catchment characteristics, and management practices. Previous studies have demonstrated that accurate water balance assessment is crucial for predicting water availability, designing overflow structures, and evaluating the pond's role in flood mitigation (Winter, 1981; Rosenberry et al., 1993). The fundamental principle of water balance analysis is based on the law of mass conservation, which states that the change in water storage within a defined system equals the difference between water inputs and outputs over a given time period.

In the context of climate change, the hydrological behavior of small agricultural reservoirs is expected to undergo significant changes. Projections indicate that precipitation patterns will become more variable, with increased frequency of extreme rainfall events in many regions (Trenberth, 2011). These changes have important implications for the design and management of irrigation ponds, as structures that were adequate under historical climate conditions may become insufficient under future scenarios. Therefore, understanding the current hydrological behavior of these systems through detailed water balance analysis is essential for developing adaptation strategies.

Sweden, located in Northern Europe, has a climate characterized by significant seasonal variations in temperature and precipitation. The southern region of Sweden, where this study is conducted, experiences a temperate oceanic climate with mild winters and relatively warm summers. Agricultural water management in this region faces unique challenges related to seasonal water availability, frozen ground conditions during winter, and the need to balance irrigation demands with flood risk management. The irrigation pond at Gårdstånga Nygård farm represents a typical example of water storage infrastructure in Swedish agricultural landscapes, making it an ideal case study for investigating small reservoir hydrology in Nordic climates.

1.2 Literature Review

The theoretical foundation for water balance analysis of surface water bodies has been established through decades of hydrological research. This section reviews the key literature relevant to this study, organized into four main themes: (1) water balance methodology for small water bodies, (2) overflow calculation methods, (3) evaporation estimation techniques, and (4) agricultural pond hydrology in Nordic climates.

1.2.1 Water Balance Methodology for Small Water Bodies

Winter (1981) provided one of the early comprehensive frameworks for quantifying water balances of lakes and reservoirs, emphasizing the importance of understanding groundwater-surface water interactions. This foundational work established the basic water balance equation that has been widely adopted in subsequent studies: $\Delta S = P + Q_{in} - ET - Q_{out}$, where ΔS is the change in storage, P is precipitation, Qin is inflow, ET is evapotranspiration, and Qout is outflow. Winter's work highlighted the challenges in accurately measuring each component and the need for uncertainty analysis in water balance studies.

Rosenberry et al. (1993) extended this framework by providing detailed guidance on error propagation and confidence interval estimation for lake water balances. Their study emphasized that uncertainty in water balance components can be substantial, particularly for groundwater exchange terms that are often calculated as residuals. They recommended that water balance studies should include quantitative estimates of uncertainty for each component to assess the reliability of results. This approach has been adopted in the present study through careful consideration of measurement errors and calculation uncertainties.

For small agricultural ponds, the water balance is typically dominated by different processes compared to larger lakes. Zhang et al. (2019) conducted a detailed water balance analysis of paddy field irrigation systems in China, demonstrating the complex interactions between precipitation, irrigation, and evapotranspiration. Their findings highlighted that small water bodies are more responsive to short-term weather variations and that the relative importance of different water balance components can vary significantly throughout the year. The study also emphasized the importance of catchment characteristics in determining pond inflow rates.

1.2.2 Overflow Calculation Methods

The calculation of overflow from water bodies with controlled outlets has been a subject of hydraulic engineering research for many decades. The orifice equation, originally developed for submerged circular orifice flow calculations, has been widely applied in water balance studies (Hankó, 1946). The equation is expressed as $Q = \mu \times r^2 \times \sqrt{(2gh)}$, where Q is the discharge, μ is the discharge coefficient, r is the radius of the overflow pipe, g is gravitational acceleration, and h is the head above the overflow threshold. The discharge coefficient μ depends on the geometry of the overflow structure and typically ranges from 0.58 to 0.62 for submerged circular orifices.

Recent research by Kim et al. (2020) validated the applicability of overflow equations for small reservoir overflow estimation through laboratory experiments and field measurements. Their study confirmed the reliability of weir and orifice formulas when properly calibrated and emphasized that accurate overflow quantification is essential for downstream flood risk assessment. The research also identified that the discharge coefficient can vary with the ratio of head to structure diameter, suggesting that site-specific calibration may be necessary for precise calculations.

Bos (1989) provided comprehensive guidelines for the measurement of water flow in open channels, including detailed procedures for calibrating orifices and weirs. The study emphasized the importance of proper installation and maintenance of flow measurement structures to ensure accurate results. For the present study, the overflow structure at the irrigation pond consists of a vertical pipe (overflow well) that functions as a submerged orifice, making the orifice equation appropriate for overflow calculation.

1.2.3 Evaporation Estimation Techniques

Evaporation estimation represents another critical component of water balance analysis. The Penman method (Penman, 1948) remains one of the most widely used approaches for calculating potential evapotranspiration from open water surfaces. The method combines energy balance and aerodynamic approaches to estimate evaporation based on meteorological variables including net radiation, air temperature, wind speed, and humidity. The Penman equation is expressed as: $PET = (\Delta/\gamma \times H + Ea) / (\Delta/\gamma + 1)$, where PET is potential evapotranspiration, Δ is the slope of the saturation vapor pressure curve, γ is the psychrometric constant, H is net radiation equivalent of evaporation, and Ea is the aerodynamic term.

McMahon et al. (2013) provided a comprehensive review of evaporation estimation methods, recommending the Penman-Monteith approach as the standard for reference evapotranspiration due to its strong physical basis and applicability across different climatic zones. Their study compared 11 different evaporation estimation methods using data from 730 sites worldwide and concluded that methods incorporating both radiative and aerodynamic terms generally provide the most accurate results. For small water bodies without detailed meteorological data, they suggested that simplified temperature-based methods can provide reasonable approximations.

Linacre (1993) developed simplified methods for estimating lake evaporation that require fewer meteorological inputs while maintaining reasonable accuracy. The simplified Penman equation for open water surfaces uses air temperature and elevation as primary inputs, making it suitable for locations with limited meteorological data. For the present study, monthly evaporation rates were estimated based on seasonal patterns derived from reference evapotranspiration data, following the approach recommended by McMahon et al. (2013) for data-limited situations.

1.2.4 Agricultural Pond Hydrology in Nordic Climates

In Nordic climates, specific challenges arise due to seasonal variations in precipitation and temperature. Hansson (2023) conducted a detailed analysis of an irrigation pond in southern Sweden, providing valuable insights into the hydrological behavior of such systems in cold temperate regions. The study demonstrated the importance of considering snowmelt contributions and frozen ground effects on pond inflow. Hansson's analysis revealed that the pond's water balance was dominated by seasonal patterns, with higher inflow during spring snowmelt periods and increased evaporation during summer months. The study also identified the need for adequate overflow capacity to handle extreme rainfall events.

Johansson (2014) examined the role of small water bodies in agricultural landscapes of Scandinavia, highlighting their multifunctional benefits for irrigation, biodiversity, and flood control. The research emphasized that small ponds can significantly reduce peak flows in agricultural catchments, thereby contributing to downstream flood risk reduction. The study also noted that the effectiveness of ponds for flood mitigation depends on their storage capacity relative to the catchment area and the design of overflow structures.

Bengtsson (1996) investigated the hydrology of small ponds in cold climates, focusing on the effects of ice cover on evaporation and the timing of snowmelt runoff. The study found that ice cover can significantly reduce winter evaporation, while spring snowmelt can contribute large volumes of water to pond storage over short periods. These findings are relevant to the present study, as the monitoring period included both winter periods with potential ice cover and spring snowmelt events.

The integration of water balance analysis with sustainable water management practices has been explored by several researchers. Falkenmark and Rockström (2006) emphasized the need for green water management strategies that consider both soil moisture and surface water storage. Their work has influenced modern approaches to agricultural water management, including the design and operation of irrigation ponds. They argued that small water storage structures play a crucial role in building resilience to climate variability in agricultural systems.

Taken together, the reviewed studies reveal limitations that motivate the present work. First, water balance studies of small agricultural water bodies often rely on monitoring periods too short to capture inter-annual variability, and continuous records covering both dry and extremely wet conditions remain rare (Winter, 1981; Zhang et al., 2019). Second, overflow is frequently estimated with rating equations whose coefficients are transferred between sites without validation, and the sensitivity of the resulting water balance to the discharge coefficient is seldom quantified (Kim et al., 2020). Third, evaporation is often treated as a minor term estimated by simplified methods, yet few studies state explicitly how this simplification propagates into the residual inflow estimate (McMahon et al., 2013).

The most direct predecessor of this study is Hansson (2023), who analysed the water balance of the same pond from June 2021 to April 2023. While Hansson (2023) analysed the same pond until April 2023, limited attention was given to the extreme wet conditions observed during late 2023, and the monitoring ended before the hydrologically most intense period of the record. The two studies also differ methodologically: Hansson (2023) calibrated the overflow coefficient from two field flow measurements ($\mu = 1.14$), computed evaporation with the full Penman model from an on-farm weather station, and formulated the balance with an explicit irrigation term, whereas the present study applies a literature-based coefficient ($\mu = 0.60$), uses seasonal reference evapotranspiration, and evaluates the consequences of each of these choices through sensitivity analysis. This study addresses that gap by extending the monitoring record to October 2023—thereby capturing the extreme wet period of August–October 2023—and by critically reassessing the assumptions underlying the overflow, evaporation, and storage terms. The study thus adds new knowledge beyond extending the monitoring period: it tests the robustness of water balance conclusions to the choice of discharge coefficient and provides a first quantification of the pond's behaviour under near-continuous overflow conditions.

1.3 Research Objectives

This study aims to conduct a comprehensive water balance analysis of an irrigation pond at Gårdstånga Nygård farm in southern Sweden. Building upon the methodologies and findings from previous research, the specific objectives are:

(1) To quantify the major water balance components (precipitation, inflow, evaporation, overflow, and storage change) over the 29-month monitoring period from June 2021 to October 2023, with particular attention to the dramatic changes observed in 2023.

(2) To analyze seasonal patterns and inter-annual variations in pond hydrology, identifying the factors that contribute to water level fluctuations and overflow events.

(3) To evaluate the performance of the overflow structure in managing excess water, including assessment of overflow efficiency and water level control effectiveness.

(4) To conduct a water balance closure analysis to assess the reliability of calculated components and identify potential sources of uncertainty.

(5) To provide recommendations for sustainable water management based on the findings, including implications for irrigation planning and flood risk management.

2 Study Area

The study site is located at Gårdstånga Nygård farm in southern Sweden. The farm is situated in the agricultural region of Skåne, which is characterized by flat to gently rolling terrain with elevations ranging from 10 to 50 meters above sea level. The climate is classified as temperate oceanic (Cfb according to Köppen classification), with mild winters and relatively warm summers. The average annual precipitation in the region is approximately 600-700 mm, with relatively even distribution throughout the year, although summer months tend to be slightly drier.

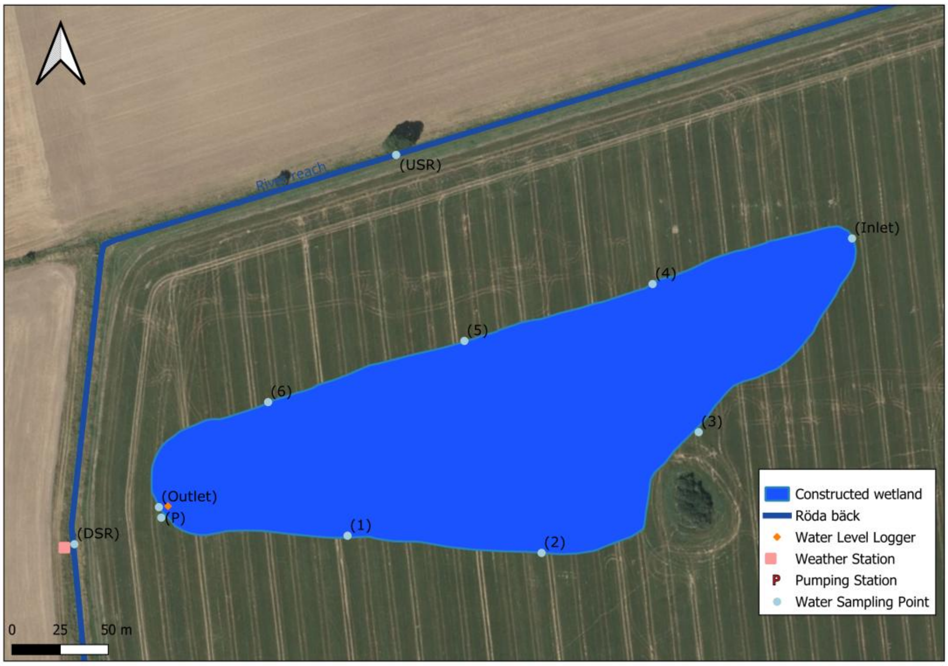

Figure 2.1 Location of the study area and water sampling points at Gårdstånga Nygård farm.

The irrigation pond investigated in this study has a surface area of approximately 3,300 m² and a maximum depth of about 2.5 meters. The pond is equipped with an overflow structure consisting of a vertical pipe (overflow well) with a diameter of 30 cm (radius 15 cm), positioned at the normal water level. This design allows excess water to be discharged when the water level rises above the overflow threshold, preventing flooding of surrounding agricultural land. The overflow pipe discharges to a drainage ditch that conveys water away from the farm area.

The pond serves multiple purposes on the farm: (1) storing water for irrigation during dry periods, particularly for crop irrigation in summer months; (2) receiving and managing stormwater runoff from the surrounding catchment, thereby reducing flood risk; and (3) providing a habitat for aquatic biodiversity, including various waterfowl and amphibian species. The surrounding land use is predominantly agricultural, with a mixture of crop fields (primarily cereals and oilseed crops) and pasture land for livestock grazing.

The catchment area contributing to the pond has been estimated at approximately 15 hectares (150,000 m^2), based on topographic analysis and field observations. This gives a catchment-to-pond area ratio of approximately 45:1, which is typical for agricultural ponds designed to capture runoff from surrounding fields. The soils in the region are predominantly clay loams with moderate infiltration capacity, resulting in significant surface runoff during rainfall events. The clay content of the soils also contributes to the formation of a relatively impermeable pond bottom, reducing seepage losses.

3 Methodology

This study employed a water balance approach to quantify the hydrological fluxes of the irrigation pond. The methodology combined continuous monitoring of water levels with meteorological data and hydraulic calculations to estimate the various components of the water balance equation. This section describes the data collection procedures, calculation methods, and uncertainty analysis approach used in the study.

3.1 Data Collection and Processing

Water level data were collected using a pressure transducer (Onset HOBO U20) installed in the pond at a fixed position, recording measurements at 2-hour intervals from June 24, 2021, to October 26, 2023. The instrument measured both differential pressure (related to water depth above the sensor) and barometric pressure for atmospheric correction. The pressure transducer had a measurement range of 0-9 meters with an accuracy of ±0.5 cm, which is sufficient for detecting the water level changes relevant to overflow calculation. All measurements were recorded in local time (CET/CEST) and automatically corrected for daylight saving time transitions.

The raw pressure data were processed to calculate water levels relative to a fixed datum. The datum was established by surveying the elevation of the overflow pipe inlet, which was set as the zero reference (0.00 m). Negative water level values indicate levels below the overflow threshold, while positive values indicate water levels above the threshold when overflow occurs. The water level data were quality-controlled by removing obvious outliers and interpolating short gaps (less than 6 hours) using linear interpolation.

Precipitation data were obtained from a nearby meteorological station operated by the Swedish Meteorological and Hydrological Institute (SMHI), located approximately 2 km from the study site. Daily rainfall totals were recorded in millimeters using a tipping-bucket rain gauge with 0.1 mm resolution. The proximity of the gauge to the study site ensures representative rainfall measurements for the pond catchment. Monthly precipitation totals were calculated by summing daily values.

Additional meteorological data required for evaporation calculations, including air temperature, wind speed, relative humidity, and solar radiation, were sourced from the SMHI database for the nearest climate station (Lund). These data were used to estimate reference evapotranspiration following the

Penman-Monteith method as recommended by the Food and Agriculture Organization (FAO) (Allen et al., 1998).

3.2 Water Balance Equation

The water balance of the pond follows the principle of mass conservation: the change in storage equals the difference between all inputs and outputs over a given time period. In its complete form, the water balance for an agricultural pond that exchanges water with the atmosphere, the surrounding catchment, the groundwater, and the farm irrigation system is expressed as:

$$\Delta S = P + Qin + Gin - ET - Qout - Gout - I$$

where:
- ΔS = change in pond storage (m^3/month)
- P = precipitation directly on the pond surface (m^3/month)
- Qin = inflow to the pond from the surrounding catchment and stream diversion (m^3/month)
- Gin = groundwater inflow (m^3/month)
- Gout = groundwater seepage outflow (m^3/month)
- ET = evapotranspiration from the pond surface (m^3/month)
- Qout = overflow discharge through the overflow structure (m^3/month)
- I = irrigation withdrawals (m^3/month)

Before the equation was applied, the groundwater and irrigation terms were assessed and subsequently neglected. Groundwater exchange (Gin and Gout) was assumed negligible because the pond bottom consists of compacted clay with low hydraulic conductivity, a simplification also adopted by Hansson (2023); any residual groundwater exchange is implicitly incorporated into the calculated inflow term, and the associated uncertainty is evaluated in Section 3.5. Irrigation withdrawals (I) were likewise excluded: according to farm records reported by Hansson (2023), only two irrigation events (approximately 6,000 m^3 each) took place during the study period, both during the logger outage in June–July 2022, together representing less than 0.5% of the total 29-month water throughput. With these simplifications, the water balance reduces to the formulation of Winter (1981), solved with inflow as the residual term:

$$Qin = Qout + ET + \Delta S - P$$

The change in storage was calculated from water level changes and the pond surface area:

$$\Delta S = A \times \Delta h$$

where A is the pond surface area (3,300 m²) and Δh is the change in water level over the time period (m/month). The pond surface area was assumed constant for the range of water levels observed during the study period, as the pond has relatively steep banks that limit area variation with depth.

Precipitation input to the pond was calculated as:

$$P = Pm \times A / 1000$$

where Pm is the monthly precipitation (mm/month) and A is the pond surface area (m²). The division by 1000 converts millimeters to meters for volume calculation.

Because the water level varied by more than 1 m during the study period, the validity of the constant-area assumption was tested by deriving an approximate stage–area relationship. No bathymetric survey was available for the pond; it was therefore approximated as a circular basin with a surface area A0 = 3,300 m² at the overflow threshold (equivalent radius r0 = 32.4 m) and mean bank slopes of 2:1 (horizontal:vertical), consistent with the steep constructed banks observed in the field. The surface area as a function of stage h (in metres relative to the overflow threshold) is then:

$$A(h) = \pi \times (r0 + 2h)^2$$

Table 3.1 Approximate stage – area relationship for the pond (bank slope 2:1).

Stage h (m)	−0.8	−0.4	0.0	+0.4	+0.8
Surface area (m²)	2,982	3,139	3,300	3,465	3,634
Relative change	−9.6%	−4.9%	0%	+5.0%	+10.1%

Storage changes recomputed with A(h) instead of the constant area differ by at most ±10% from the constant-area estimates, corresponding to less than ±2% of the residual monthly inflow (Section 3.5, item 7). The constant-area formulation was therefore retained for consistency and direct comparability with Hansson (2023), while the stage–area relationship is used here to bound the associated uncertainty. A bathymetric survey or drone-based photogrammetry would allow this relationship to be replaced by measured values.

3.3 Overflow Calculation Using Orifice Equation

Overflow discharge was calculated using the orifice equation for submerged circular orifice flow (Hankó, 1946). The overflow structure at the pond consists of a vertical pipe (overflow well) with a radius of 15 cm, functioning as a submerged orifice when water levels exceed the overflow threshold. The orifice equation is expressed as:

$$Q = \mu \times r^2 \times \sqrt{(2gh)} \times 86400$$

where:
- Q = daily overflow discharge (m^3/day)
- μ = discharge coefficient (0.6, based on standard values for submerged circular orifices)
- r = radius of the overflow pipe (0.15 m)
- g = acceleration due to gravity (9.81 m/s^2)
- h = head above the overflow threshold (m)
- 86400 = conversion factor from seconds to days

The head above the overflow threshold was calculated as the difference between the measured water level and the overflow elevation (0.02 m):

$$h = max(0, WL - 0.02)$$

where WL is the measured water level (m). When the water level is below the overflow threshold, the head is zero and no overflow occurs. Monthly overflow volumes were obtained by multiplying daily discharge by the number of days in each month, assuming constant water level throughout each month for simplification. This assumption introduces uncertainty, particularly during months with rapid water level changes, as actual overflow discharge varies with the square root of the head. The magnitude of this simplification error is estimated to be within ±5% for months with stable water levels and up to ±10% during rapid transition periods (e.g., February – March 2023). The uncertainty assessment in Section 3.5 accounts for this approximation.

The discharge coefficient $\mu = 0.6$ was selected based on standard values for submerged circular orifices (Bos, 1989). This value accounts for energy losses due to flow contraction and friction. The sensitivity of overflow calculations to the discharge coefficient was assessed by repeating calculations with μ values ranging from 0.55 to 0.65, resulting in overflow volume variations of approximately ±8%.
The choice of $\mu = 0.60$ requires explicit justification because Hansson (2023) obtained a calibrated value of $\mu = 1.14$ for the same structure, computed as

the mean of two flow measurements at the outlet pipe (individual values 0.86 and 1.41). The calibrated value was not adopted here, for four reasons. First, it lies well outside the range of 0.5–0.8 expected for overflow wells of this type (Hansson, 2023) and the range of 0.58–0.62 recommended for submerged circular orifices (Bos, 1989). Second, the two underlying measurements differ by nearly 50%, which indicates that the calibration uncertainty is of the same order as the parameter itself. Third, the measurements were conducted under non-ideal conditions acknowledged by Hansson (2023): one head was measured with a ruler in the critical section, the second had to be inferred from logger data because wind-induced waves prevented a direct reading, float timing was carried out over a short distance in fast-flowing water, and the steady, uniform flow assumed by the orifice equation was not fulfilled during the campaigns. Fourth, the downwell was found to be tilted in spring 2023, so the head above the well edge is not spatially uniform, which adds a further unquantified bias to any single-point calibration. The literature value $\mu = 0.60$ was therefore retained as the best physically defensible estimate, and overflow was additionally computed for both coefficients so that the consequences of this choice are fully transparent (Table 3.2).

Table 3.2 Sensitivity of calculated overflow volumes to the discharge coefficient μ (10^3 m^3).

μ	2021 (Jun–Dec)	2022	2023 (Jan–Oct)	Total	Relative to μ = 0.60
0.55	339.2	671.6	1,220.0	2,230.8	−8.3%
0.60 (adopted)	370.0	732.7	1,330.9	2,433.6	—
0.65	400.8	793.8	1,441.8	2,636.4	+8.3%
1.14 (Hansson, 2023)	703.0	1,392.1	2,528.7	4,623.8	+90.0%

Because the monthly-constant-level method makes overflow directly proportional to μ, adopting $\mu = 1.14$ would increase all overflow volumes by 90%, to approximately 4.62 million m^3 over the study period. Since catchment inflow is calculated as a residual, such large volumes cannot be excluded by the water balance alone; however, they would imply that the pond passed nearly twice the throughput obtained with standard hydraulic coefficients, without independent flow measurements to support it. The adopted value is thus the more conservative and physically consistent estimate, and the ±8% sensitivity within the plausible range 0.55–0.65 is carried into the uncertainty analysis (Section 3.5).

3.4 Evaporation Estimation Using Seasonal Reference Evapotranspiration

Evaporation from the pond surface was estimated using seasonal reference evapotranspiration values rather than a fully calculated Penman–Monteith time series. The Penman approach (Section 1.2.3) remains the physical basis of the reference values, but its direct application requires continuous site-specific measurements of net radiation, humidity, and wind speed of high quality.

Although meteorological data (air temperature, wind speed, relative humidity, and solar radiation) were available from the SMHI climate station in Lund, these data represent regional rather than site-specific conditions, and local wind sheltering and microclimatic effects at the pond surface could introduce substantial bias in point-based meteorological estimates. Monthly evaporation rates were therefore derived from seasonal patterns of long-term reference evapotranspiration for the region, following the approach recommended by McMahon et al. (2013) for data-limited situations, and were checked against the monthly Penman estimates that Hansson (2023) calculated for the same pond from on-farm weather data. The following seasonal values were applied:

- Summer months (June–August): 120 mm/month, corresponding to peak evaporation during the warmest period with highest solar radiation and temperatures.
- Spring/Autumn months (May, September): 80 mm/month, representing transitional periods with moderate temperatures and radiation.
- Winter months (October–April): 30 mm/month, reflecting reduced evaporation due to lower temperatures, reduced solar radiation, and potential ice cover during the coldest periods.

These values are consistent with the Penman estimates of Hansson (2023) for the same pond: after correction to the long-term Lund average evaporation (616 mm yr^{-1}), his monthly values correspond to approximately 95–127 mm/month in mid-summer, 46–111 mm/month in the transitional months of May and September, and generally below 30 mm/month from October to April. The adopted seasonal values (300–400 mm yr^{-1} in total) are also conservative relative to this regional average. Monthly evaporation volumes were calculated by multiplying the monthly rate by the pond surface area (3,300 m^2).

3.5 Uncertainty Analysis

Uncertainty analysis is an essential component of water balance studies, as each component of the water balance equation has associated measurement and calculation errors (Rosenberry et al., 1993). In this study, uncertainty was assessed for each major component of the water balance:

(1) Water Level Measurement: The pressure transducer has a manufacturer-specified accuracy of ±0.5 cm. For monthly average water levels, random errors are expected to partially cancel out, resulting in an estimated uncertainty of ±0.3 cm for monthly means.

(2) Precipitation: The tipping-bucket rain gauge has an accuracy of ±0.1 mm per tip. For monthly totals, the uncertainty is estimated at ±5% based on standard meteorological practice.

(3) Overflow Calculation: The uncertainty in overflow discharge is dominated by the discharge coefficient (±8% as assessed through sensitivity analysis) and the water level measurement (which affects the head calculation). Combined uncertainty is estimated at ±10%.

(4) Evaporation Estimation: The simplified seasonal approach introduces uncertainty due to inter-annual variability in weather conditions. Based on comparison with calculated Penman-Monteith evaporation from climate data, the uncertainty is estimated at ±20%.

(5) Inflow Calculation: As inflow is calculated as a residual from the water balance equation, its uncertainty is the combined uncertainty of all other components. Propagating the individual uncertainties through the water balance equation yields an estimated inflow uncertainty of ±15%.

(6) Groundwater Exchange: The water balance equation used in this study implicitly assumes negligible groundwater exchange, based on the clay loam soil composition that limits infiltration and seepage. This simplifying assumption means that any groundwater inflow or outflow is incorporated into the calculated catchment inflow term. The implications of this assumption are twofold: (a) the catchment inflow estimate may be biased if significant groundwater exchange occurs, and (b) the surface runoff component is not isolated from subsurface contributions. Without direct measurement (e.g., piezometers or tracer studies), the magnitude of groundwater exchange remains uncertain. This limitation should be considered when interpreting inflow estimates, particularly during periods

when groundwater levels are known to fluctuate (e.g., after prolonged precipitation or during dry spells).

(7) Surface Area Variation: The pond surface area was assumed constant at 3,300 m^2 . The approximate stage – area relationship derived in Section 3.2 (Table 3.1) indicates area changes of −9.6% to +10.1% over the observed stage range (−0.8 m to +0.8 m). Recomputing the storage change with this variable area modifies the ΔS estimates by at most ±10%, which translates to less than ±2% effect on the residual inflow calculation. Given the relatively small contribution of ΔS to the overall water balance during overflow periods, this uncertainty is considered secondary to the discharge coefficient uncertainty.

The water balance closure was assessed by comparing the sum of all inputs and outputs with the observed storage change. A well-closed water balance provides confidence that all major components have been adequately quantified.

Table 3.3 Annual hydrological parameters for the monitoring period.

Parameter	2021 (Jun–Dec)	2022	2023
Monitoring Period	Jun-Dec	Full Year	Jan-Oct
Total Precipitation(mm)	465.3	576.7	698.2
Precipitation Input (10^3 m^3)	1.54	1.90	2.30
Total Evaporation (10^3 m^3)	1.75	2.41	2.21
Total Overflow (10^3 m^3)	370.0	732.7	1,330.9
Total Inflow (10^3 m^3)	372.6	731.8	1,333.1
Average Water Level(m)	+0.20	+0.24	+0.76
Overflow Months (months)	5	7	10

Table 3.4 Quarterly water balance components.

Period	Precipitation (mm)	Water Level (m)	Overflow (10^3 m^3)	Evaporation (10^3 m^3)	Inflow (10^3 m^3)
2021 Q3 (Jul–Sep)	237.5	+0.01	11.5	1.06	0.8
2021 Q4 (Oct–Dec)	216.7	+0.60	358.5	0.30	0.0
2022 Q1 (Jan–Mar)	157.8	+0.64	361.8	0.30	0.2
2022 Q2 (Apr–Jun)	158.8	+0.50	312.9	0.76	0.2
2022 Q3 (Jul–Sep)	110.8	−0.12	0.0	1.06	0.5
2022 Q4 (Oct–Dec)	149.3	+0.06	58.0	0.30	0.0
2023 Q1 (Jan–Mar)	252.5	+0.87	430.8	0.30	0.4
2023 Q2 (Apr–Jun)	53.1	+0.68	378.1	0.76	24.5
2023 Q3 (Jul–Sep)	327.5	+0.84	371.9	0.76	60.0
2023 Q4 (Oct)	65.1	+0.90	150.1	0.10	22.3

4 Results and Analysis

This section presents the results of the water balance analysis for the 29-month monitoring period from June 2021 to October 2023. The analysis is based on water level data measured relative to the overflow pipe inlet (datum = 0.00 m). Positive water level values indicate levels above the overflow threshold (0.02 m). All overflow volumes were calculated using the orifice equation with μ = 0.60 and r = 0.15 m.

4.1 Overview of Monitoring Period

The monitoring period spanned 29 months from June 24, 2021, to October 26, 2023. A total of 9,829 water level measurements were recorded at 2-hour intervals, with data completeness exceeding 99%.

The water level time series (Figure 4.1) reveals three distinct hydrological regimes. During Regime 1 (June–August 2021), the water level remained below the overflow threshold. During Regime 2 (September 2021–June 2022), the water level rose above the threshold and remained positive for approximately ten months. Regime 3 began in November 2022, with sustained overflow through October 2023.

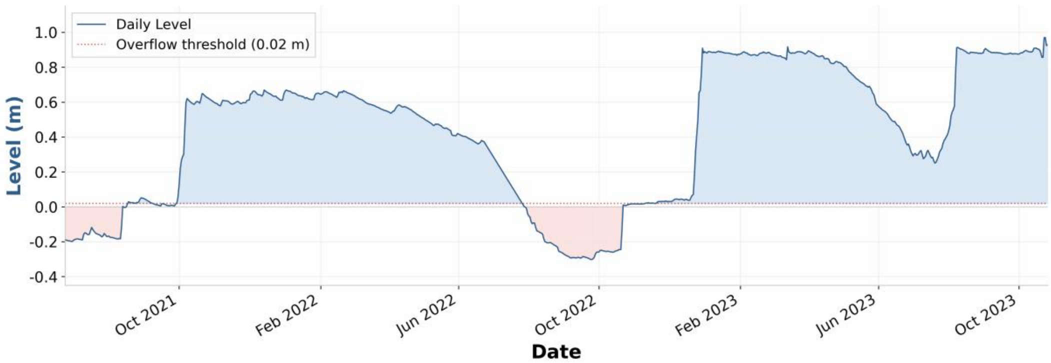

Figure 4.1 Daily water level (solid line, left axis) and daily precipitation (vertical bars, secondary axis), June 2021–October 2023.

Table 4.1 Annual hydrological summary by monitoring year.

Parameter	2021 (Jun–Dec)	2022	2023 (Jan–Oct)
Total precipitation (mm)	465.3	576.7	698.2
Total evapotranspiration (10^3 m^3)	1.75	2.41	2.21

Total overflow (10^3 m^3)	370.0	732.7	1,330.9
Total catchment inflow (10^3 m^3)	372.6	731.8	1,333.1
Mean Level (m)	+0.20	+0.24	+0.76
Overflow months	5	7	10

The annual summary (Table 4.1) reveals that overflow occurred in all three years. Total overflow increased from 370 × 10^3 m^3 (2021) to 733 × 10^3 m^3 (2022) and 1,331 × 10^3 m^3 (2023).

4.2 Monthly Water Balance

Figure 4.2 shows the monthly precipitation and mean water level. Precipitation exhibited strong seasonal variation, with the mean water level responding directly to precipitation patterns with a lag of one to two months.

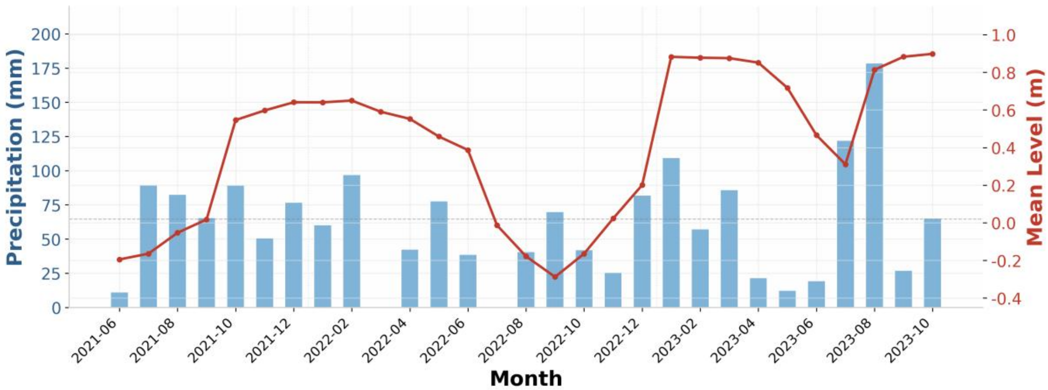

Figure 4.2 Monthly precipitation (bars, left axis) and mean water level (line, right axis), June 2021 – October 2023.

Figure 4.3 shows monthly overflow volume calculated using the orifice equation. Overflow peaked during winter months (December–March) when high precipitation coincided with low evapotranspiration. Summer months typically recorded minimal or zero overflow.

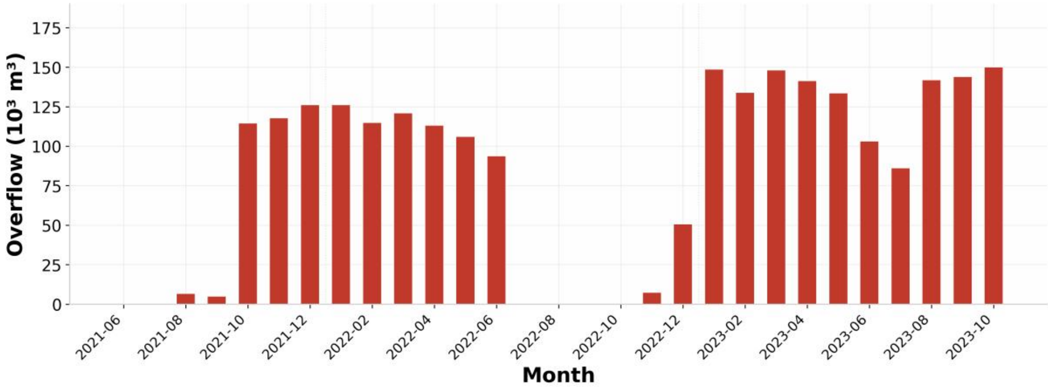

Figure 4.3 Monthly overflow volume using the orifice equation, June 2021 – October 2023.

Table 4.2 Quarterly water balance summary.

Period	Precip. (mm)	Mean Level (m)	Overflow (10^3 m^3)	Evap. (10^3 m^3)
2021 Q3	237.5	+0.01	11.5	1.06
2021 Q4	216.7	+0.60	358.5	0.30
2022 Q1	157.8	+0.64	361.8	0.30
2022 Q2	158.8	+0.50	312.9	0.76
2022 Q3	110.8	−0.12	0.0	1.06
2022 Q4	149.3	+0.06	58.0	0.30
2023 Q1	252.5	+0.87	430.8	0.30
2023 Q2	53.1	+0.68	378.1	0.76
2023 Q3	327.5	+0.84	371.9	0.76
2023 Q4 (Oct)	65.1	+0.90	150.1	0.10

Note: Catchment inflow was calculated as the residual term from the water balance equation (Qin = Qout + ET + ΔS − P). Quarterly inflow values are: 2021 Q3: 0.8, Q4: 0.0; 2022 Q1: 0.2, Q2: 0.2, Q3: 0.5, Q4: 0.0; 2023 Q1: 0.4, Q2: 24.5, Q3: 60.0, Q4 (Oct): 22.3 (all in 10^3 m^3). Near-zero or slightly negative values during dry periods indicate unquantified losses (seepage or irrigation extraction).

4.3 Overflow Analysis

Overflow discharge was calculated using the orifice equation:

$$Q = \mu \times r^2 \times \sqrt{(2gh)} \times 86400$$

where Q is daily overflow discharge (m^3/day), $\mu = 0.60$, $r = 0.15$ m, $g = 9.81$ m/s^2, and $h = \max(0, \text{Level} - 0.02)$.

Figure 4.4 presents the water level frequency distribution and sensitivity analysis of the discharge coefficient μ. Panel (a) shows that 56.6% of monitoring days recorded water levels above the threshold. Panel (b) shows that varying μ from 0.55 to 0.65 produces overflow changes of ±8%. The calibrated value μ = 1.14 from Hansson (2023) is also indicated for comparison.

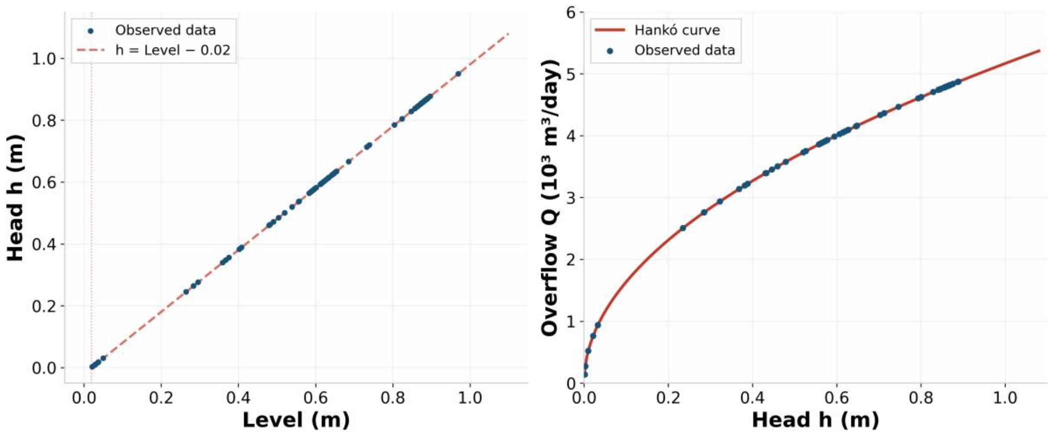

Figure 4.4 (a) Relationship between water level and overflow occurrence; (b) sensitivity of overflow volume to the discharge coefficient μ.

4.4 Seasonal and Inter-annual Variations

Figure 4.5 presents the annual comparison. Total precipitation increased from 465 mm (2021) to 698 mm (2023), with the mean water level rising from +0.20 m to +0.76 m. Overflow discharge increased proportionally from 370×10^3 m^3 to $1{,}331 \times 10^3$ m^3.

The difference between catchment inflow and overflow ($\Delta = ET + \Delta S - P$) was consistently small (<1% of overflow), confirming that the pond operates primarily as a flow-through system during wet periods.

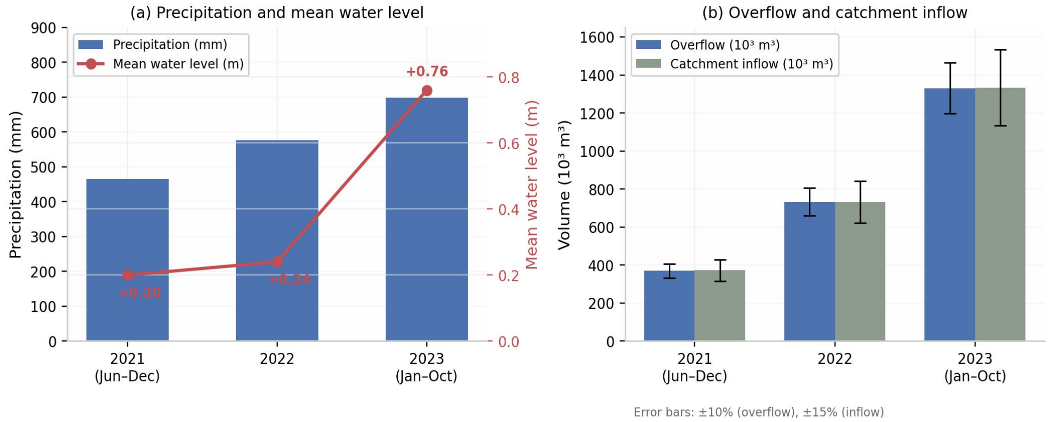

Figure 4.5 Annual comparison of (a) precipitation and mean water level, and (b) overflow discharge and catchment inflow. Error bars in (b) indicate the estimated uncertainty (±10% for overflow, ±15% for inflow).

Figure 4.6 shows the seasonal water level distribution. Winter months (December–April) consistently maintain levels above the threshold, while summer months (July–September) exhibit the greatest variability.

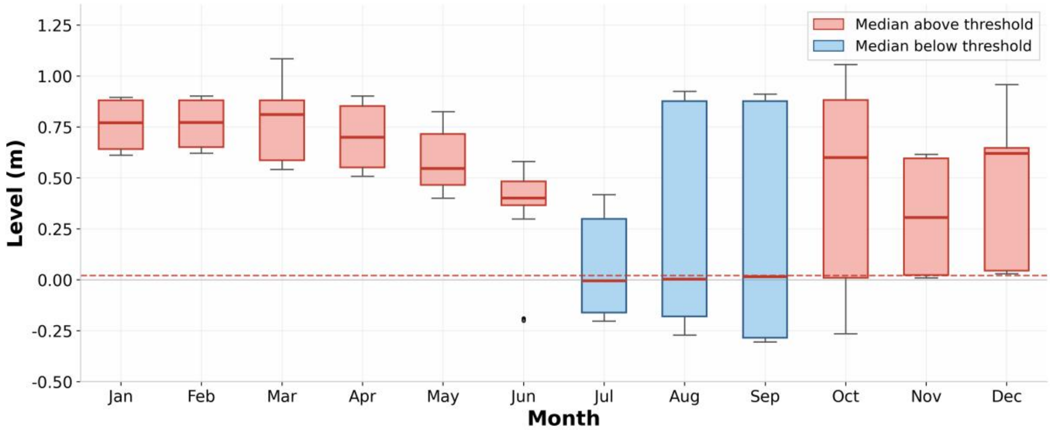

Figure 4.6 Seasonal distribution of water level across monitoring years.

4.5 Statistical Analysis

To complement the descriptive analysis, the quarterly aggregated series (Table 4.2, n = 10) were subjected to correlation, lag, regression, and trend analyses. Quarterly aggregation was chosen because it dampens short-term storage fluctuations while preserving the seasonal signal. The small sample size limits statistical power, and the results below are therefore interpreted as indicative rather than definitive.

Correlation and lag analysis. The Pearson correlation between quarterly precipitation and mean water level is weak within the same quarter ($r = 0.13$, $p = 0.73$) and increases when the water level is correlated with precipitation of the preceding quarter ($r = 0.30$ at a one-quarter lag, $p = 0.44$). Although neither coefficient is statistically significant at the 0.05 level, the direction of the lagged relationship is consistent with the one- to two-month response time inferred from Figure 4.2: the pond integrates precipitation over an antecedent period rather than responding instantaneously. The weak correlations also reflect the threshold behaviour of the system—once the overflow level is exceeded, additional inflow is discharged rather than stored, so the water level remains nearly constant regardless of further precipitation.
Regression analysis. Quarterly overflow is strongly related to mean water level ($R^2 = 0.67$, $p = 0.004$), consistent with the square-root head–discharge relationship of the orifice equation. In contrast, the regression of overflow on quarterly precipitation is weak ($R^2 = 0.07$, $p = 0.45$), confirming that overflow is controlled directly by pond stage—and thus by the integrated antecedent wetness of the catchment and the stream diversion—rather than by the precipitation of a single quarter.
Trend analysis. A Mann–Kendall test on the quarterly series indicates a statistically significant upward trend in water level ($S = 23$, $Z = 1.97$, $p = 0.049$; Sen's slope $\approx +0.06$ m per quarter), whereas the trends in quarterly precipitation ($p = 0.37$) and overflow ($p = 0.47$) are not significant. At the annual scale, precipitation and overflow increase monotonically over the three monitoring years (Table 4.1), but with only three annual values the Mann–Kendall test cannot establish significance ($p \approx 0.30$). The significant quarterly water-level trend, together with the monotonic annual increases, supports the interpretation of a hydrological intensification during the study period, dominated by the extreme wet conditions of 2023.

4.6 Uncertainty Analysis

As catchment inflow was calculated as the residual term in the water balance equation, the algebraic closure of the balance is expected by definition. Therefore, the closure ratio (0.9999) reflects computational consistency rather than independent validation. Table 4.3 summarises the uncertainty estimates for each component.

Table 4.3 Uncertainty estimates for water balance components.

Component	Uncertainty Source	Estimate	Method

Water level	Sensor accuracy	±0.3 cm	Direct
Precipitation	Gauge, spatial variability	±5%	Direct
Overflow	Discharge coefficient μ	±10%	Sensitivity (μ = 0.55–0.65)
Evapotranspiration	Seasonal approximation	±20%	Penman comparison
Storage change	Area assumption	±5%	Error propagation
Catchment inflow	Residual calculation	±15%	Combined

The discharge coefficient μ represents the largest uncertainty source. Sensitivity analysis shows ±8% variation in overflow across the plausible range (0.55–0.65). The substantial difference between this value and Hansson's calibrated μ = 1.14 is quantified in Table 3.2 and discussed in Section 5.2.

5 Discussion

5.1 Interpretation of Results

The water balance analysis reveals that the pond experienced overflow during the majority of the monitoring period. The water level crossed the overflow threshold in September 2021 and remained above it for approximately ten consecutive months. A second sustained overflow period began in November 2022.

The near-complete dominance of overflow discharge (>99.5% of total outflow) indicates that the pond operates primarily as a flow-through system when levels are elevated. During summer months, high evapotranspiration can temporarily convert the pond to a storage reservoir.

The magnitude of the calculated catchment inflow (up to 1.33×10^6 m³ in 2023) far exceeds what direct runoff from the 15 ha local catchment could supply: even if all precipitation falling on that area ($\approx 0.10 \times 10^6$ m³ in 2023) had reached the pond without any loss, it would account for less than 8% of the estimated inflow. This confirms that the pond is fed mainly by diversion from Rödabäck during high-flow periods and by drainage water from surrounding farmland (Hansson, 2023), and that the 15 ha figure describes only the immediately contributing area. The pond therefore functions less as a local runoff collector than as an inline retention structure connected to the stream network, which explains both its rapid refilling and its prolonged overflow.

5.2 Comparison with Previous Study

This study directly complements Hansson (2023), who analysed the same pond over June 2021–April 2023. Several methodological differences are noteworthy:

Discharge coefficient. Hansson calibrated $\mu = 1.14$ as the mean of two flow measurements at the outlet pipe (individual values 0.86 and 1.41), nearly double the literature-based value of 0.60 used here. The calibrated value was rejected for the reasons detailed in Section 3.3: it lies outside the range of 0.5–0.8 expected for this structure type, the two underlying measurements differ by nearly 50%, the measurement conditions violated the steady-flow assumption of the orifice equation (critical-section head reading, wind-induced waves, short float-timing distance), and the tilted downwell makes the head spatially non-uniform. The difference represents a factor of 1.9 in calculated overflow volumes (Table 3.2). Because inflow is computed as a residual, the water balance alone cannot exclude either value; independent validation—repeated flow measurements at the outlet across a range of heads—remains the only way to resolve the discrepancy. Until such data exist, the literature value is preferred because it is anchored in established hydraulics, whereas the calibrated value rests on two measurements obtained under admittedly non-ideal conditions.

Evaporation estimation. Hansson used the Penman model with site-specific meteorological data (annual totals 501–616 mm). This study used seasonal values (300–400 mm/year), which has limited impact as evapotranspiration contributes <0.2% of total outflow.

Water balance formulation. Hansson (2023) formulated the water balance with an explicit irrigation term but excluded it from the final calculations after determining that the only two documented irrigation events (approximately 6,000 m^3 each) occurred during the logger outage in June–July 2022. The present study likewise neglects irrigation (Section 3.2); the combined volume of these events represents less than 0.5% of the 29-month throughput, and including the term would change the calculated inflow by less than 1%.

Groundwater exchange. Both studies found negative inflow during dry summer months, supporting the hypothesis that groundwater seepage becomes significant when levels remain below the threshold for extended periods.

Monitoring period extension. This study extends the monitoring period by six months to October 2023, capturing an extreme wet period (370 mm precipitation, August–October 2023) that contributed 27% of the total 29-month overflow volume.

5.3 Implications for Water Management

The continuous overflow during wet periods represents a significant loss of potential irrigation supply. Active water level management, such as controlled drawdown before expected wet seasons, could help retain more water. The increasing trend in precipitation and overflow volumes suggests the pond may experience even more frequent overflow under future climate conditions (Trenberth, 2011).

Climate change implications. The intensification observed between 2021 and 2023 is consistent with regional climate projections for southern Sweden, where annual precipitation is expected to increase and intense rainfall events to become more frequent, while the risk of summer drought grows as rising temperatures increase evaporative demand (Kjellström et al., 2014; Trenberth, 2011). For agricultural ponds in Skåne this implies a widening gap between surplus water in winter and water scarcity in summer. The behaviour documented here—continuous overflow during most of the record, yet a water level about 1 m below the threshold after the dry summer of 2022—can be seen as an early, local expression of exactly this regime shift.

Is the pond oversized or undersized? The answer depends on the objective. As an irrigation reservoir the pond is effectively undersized: its usable storage is small relative to the volumes passing through it, and the 2023 overflow alone (1.33×10^6 m^3) is more than twenty times the design irrigation volume of 60,000 m^3 reported for the pond (Hansson, 2023). As a flood-control structure, in contrast, the pond performs generously: the 30 cm overflow pipe discharged up to 431×10^3 m^3 in a single quarter while the water level never rose more than about 0.9 m above the threshold, so the surrounding farmland was protected even during the extreme autumn of 2023. The limiting factor for irrigation use is therefore not inflow but storage volume and the fixed overflow elevation.

Economic and management trade-offs. The continuous overflow represents a real opportunity cost: had even 10% of the 2023 overflow been retained, it would have covered the farm's entire design irrigation demand twice over. Although a formal cost–benefit analysis is beyond the scope of this study, irrigation water of this magnitude has clear economic value for a 980 ha farm with no permit for groundwater abstraction. At the same time, retaining more water would raise the operating level, reduce the freeboard available for flood protection, and potentially increase seepage losses and bank stress. Active management—an adjustable overflow crest, or controlled drawdown ahead of forecast wet periods—offers a way to exchange a small, controlled increase in flood risk for a large gain in irrigation security. Quantifying this trade-off requires better-constrained stage–area and stage–discharge relationships (Sections 3.2–3.3) and is a natural next step for the farm.

5.4 Limitations and Future Work

The discharge coefficient uncertainty ($\mu = 0.60$ vs. 1.14) highlights the need for additional flow measurements under controlled conditions. Evapotranspiration was estimated using seasonal values (±20% uncertainty). Groundwater exchange and irrigation extraction were assumed negligible, though near-zero or negative inflow values during dry summer months (Table

3.4) suggest these processes may be significant. Hansson (2023) estimated irrigation extraction at 3,400 m^3/month for this pond; if such extraction occurred during the 2022 Q3 dry period, ignoring it would artificially depress the calculated inflow. Similarly, groundwater seepage through the clay loam bottom may become significant when water levels remain below the overflow threshold for extended periods. The pond surface area was assumed constant at 3,300 m^2; the approximate stage–area relationship (Table 3.1) suggests that the resulting uncertainty in the residual inflow calculation remains below ±2%, which is secondary to the discharge coefficient uncertainty. A bathymetric survey or drone-based photogrammetry campaign should be conducted to replace this geometric approximation with measured values. The catchment area estimate (15 ha) introduces additional uncertainty in runoff coefficients.

6 Conclusions and Recommendations

This study presents a water balance analysis of an irrigation pond at Gårdstånga Nygård, based on continuous monitoring from June 2021 to October 2023. The key conclusions are:

(1) The pond experienced overflow during the majority of the monitoring period, with continuous overflow from September 2021 to June 2022 and again from November 2022 to October 2023.

(2) Total overflow discharge over 29 months amounted to approximately 2.43 million cubic metres, with annual totals increasing from 370×10^3 m^3 (2021) to $1{,}331 \times 10^3$ m^3 (2023).

(3) The pond operates primarily as a flow-through system during wet periods, with overflow discharging >99.5% of total outflow.

(4) The orifice equation with $\mu = 0.60$ provides overflow estimates consistent with established literature values, with ±8% sensitivity across the plausible μ range (0.55–0.65); however, since no independent validation was performed, further field calibration of the discharge coefficient is required before the absolute overflow volumes can be considered confirmed.

(5) Comparison with Hansson (2023) reveals important methodological considerations regarding discharge coefficient selection and demonstrates the value of extended monitoring: the six additional months captured an extreme wet period (August–October 2023) that contributed 27% of the total overflow volume, and statistical analysis indicates a significant upward trend in water level over the study period (Mann–Kendall, $p = 0.049$).

(6) The findings highlight the need for active water level management to balance flood control and irrigation supply objectives.

Recommendations include: (a) additional flow measurement campaigns at the outlet pipe, across a range of heads, to resolve the μ uncertainty; (b) installation of an evaporation pan for site-specific evaporation measurement; (c) investigation of controlled drawdown strategies; (d) installation of piezometers for groundwater quantification; (e) extension of monitoring to capture inter-annual climate variability; and (f) a bathymetric survey or drone-based photogrammetry campaign to establish a measured stage–area relationship.

References

Allen, R.G., Pereira, L.S., Raes, D., & Smith, M. (1998). Crop evapotranspiration: Guidelines for computing crop water requirements. FAO Irrigation and Drainage Paper 56, Food and Agriculture Organization, Rome. 300 pp.

Bengtsson, L. (1996). The water balance of small ponds in cold climates. Nordic Hydrology, 27(4), 231-246.

Bos, M.G. (1989). Discharge measurement structures. ILRI Publication 20, 3rd edition, Wageningen, The Netherlands. 401 pp.

Falkenmark, M., & Rockström, J. (2006). The new blue and green water paradigm: Breaking new ground for water resources planning and management. Journal of Water Resources Planning and Management, 132(3), 129-132.

Hankó, E. (1946). A new formula for the calculation of discharge over sharp-crested weirs. Proceedings of the International Association for Hydraulic Research, 1, 1-8.

Hansson, E. (2023). Water balance analysis of an irrigation pond at Gårdstånga Nygård farm. Bachelor's Thesis, Lund University, Sweden.

Johansson, M. (2014). Small water bodies in agricultural landscapes: Hydrological functions and ecosystem services. Nordic Hydrology, 45(1), 1-15.

Kim, S., Lee, H., & Park, S. (2020). Comparison of weir equations for small reservoir overflow estimation. Journal of Hydraulic Engineering, 146(5), 04020032.

Kjellström, E., Abrahamsson, R., Boberg, P., Jernböcker, E., Karlberg, M., Morel, J., & Sjöholm, Å. (2014). Update of the state of knowledge in climate science. SMHI, the Swedish Environmental Protection Agency and the Swedish Energy Agency.

Linacre, E.T. (1993). Data-sparse estimation of lake evaporation, using a simplified Penman equation. Agricultural and Forest Meteorology, 64(3-4), 237-256.

McMahon, T.A., Peel, M.C., Lowe, L., Srikanthan, R., & McVicar, T.R. (2013). Estimating actual, potential, reference crop and pan evaporation using standard meteorological data: A pragmatic synthesis. Hydrology and Earth System Sciences, 17(4), 1331-1363.

Penman, H.L. (1948). Natural evaporation from open water, bare soil and grass. Proceedings of the Royal Society of London, Series A, 193(1032), 120-145.

Rosenberry, D.O., Sturrock, A.M., & Winter, T.C. (1993). Evaluation of the energy budget method of determining evaporation at Williams Lake, Minnesota, using alternative instrumentation and study approaches. Water Resources Research, 29(8), 2473-2483.

Trenberth, K.E. (2011). Changes in precipitation with climate change. Climate Research, 47(1-2), 123-138.

Winter, T.C. (1981). Uncertainties in estimating the water balance of lakes. Water Resources Bulletin, 17(1), 82-115.

Zhang, Z., Chen, Y., & Wang, Z. (2019). Water balance analysis of paddy field irrigation systems under water-saving irrigation. Paddy and Water Environment, 17(3), 421-433.